Wide-Band Waveguide and Ridge Waveguide T-Junctions for Diplexer Applications

Hui-Wen Yao, *Student Member, IEEE,* Amr E. Abdelmonem, Ji-Fuh Liang, Xiao-Peng Liang, *Student Member, IEEE,* Kawthar A. Zaki, *Fellow, IEEE,* and Alain Martin

Abstract—**Scattering parameters of E- and H-plane stepped waveguide and E-plane ridge waveguide stepped T-junctions are obtained using an extension of the three plane mode matching method [1]. An optimization process is applied to find the T-junctions and steps dimensions that yield low reflection coefficient in one of the T-junction arms over a wide frequency band. An example of the design of a wide-band T-junction diplexer is presented. The diplexer filters are inductive window waveguide filters, and are rigorously modeled using mode matching and a novel two-dimensional curve fitting method, which drastically reduces the CPU time for optimization. The diplexer optimization procedure, as well as the filter modeling method, are described. Experimental results on the optimized T-junction and the diplexer are presented; both showed excellent agreement with their computed optimum results, without any adjustments or tuning.**

I. Introduction

WAVEGUIDE T-junctions are important components in many microwave applications. Since these junctions are lossless reciprocal three ports, all three ports cannot be matched simultaneously. However, in some applications [2], it is desirable to have the T-junction with one of its ports well matched over a reasonable wide frequency band. This paper extends the three plane mode matching method [1] to the analysis and optimization of stepped waveguides and ridge waveguides T-junctions [3], to achieve wide bandwidth match of one of the ports. Analysis of the stepped structures is presented in Section II. The optimized T-junctions are used in the design of a wide bandwidth, low loss, high power diplexer. The diplexer filters are waveguide inductive iris window-type filters. In Section III, the filters are modeled rigorously by using mode matching to determine the S-parameters of the inductive windows. A two-dimensional curve fitting method is developed to reduce the required computation time. This method uses the computed mode matching S-parameters of the inductive windows, at few frequency points and window widths, to obtain two-dimensional polynomial representation of the values of the filter's circuit elements. The resulting computed filter responses are extremely accurate, and the required computation time is reduced by several orders of magnitude. The theoretical performance of the optimized T-junctions computed using mode matching is verified experimentally. Using the optimized T-junction, a network model of the diplexer with two inductive iris filters is developed. In Section III, computed filter S-parameters are used in the network model to optimize the wide-band diplexer performance. Results of the computed optimized and the measured diplexer responses are presented. The two responses agreed remarkably without further adjustment.

Manuscript received March 26, 1993; revised June 14, 1993.

H.-W. Yao, A. E. Abdelmonem, J.-F. Liang, X.-P. Liang, and K. A. Zaki are with the Electrical Engineering Department, University of Maryland, College Park, MD 20742.

A. Martin is with Mitec Electronics Ltd., 104 Gun Avenue, Pointe Claire, Q.P., Canada H9R 3X3.

IEEE Log Number 9212965.

II. Stepped Waveguide and Ridge Waveguide T-Junctions

A. Waveguide Stepped T-Junctions

Fig. 1 shows stepped E-plane and H-plane waveguide T-junctions. The junctions can be analyzed using the three plane mode matching method described in [1]. The three-port scattering matrix of the T-junction is determined from three two-port scattering matrices computed (or measured) by placing three different lengths of short circuit lines in port 3 of the T-junctions. The resulting two-port structures are treated as three lengths of different cross sections of uniform waveguides, and their scattering matrices are easily determined using mode matching. The optimum T-junctions will have minimum reflections in port 1 over the widest possible frequency band, while the power to ports 2 and 3 are divided equally. To optimize the dimensions, the S-parameters are computed as a function of frequency with b_{1B} and b_{1C} as parameters. Fig. 2 shows the computed S-parameters of an E-plane T-junction without step in the straight arm, and the width b_{1B} of port 3 as a parameter. Fig. 3 shows the computed S-parameters with the step height (or b_{1C}) as a parameter for a fixed b_{1B}. From Figs. 2 and 3, it is seen that there is an optimum dimension for the junction over the frequency band of interest. This optimum was obtained using the simple search process of the variables b_{1C} and b_{1B}. Computed and measured results for the optimum junction are shown in Fig. 4. Since the junction has only one standard waveguide port, the measured results were obtained by using three short circuits of different lengths on both ports 2 and 3, and measuring the reflection coefficient in port 1 as a function of frequency 9 times. The complete scattering matrix elements of the T-junction were extracted from these measurements.

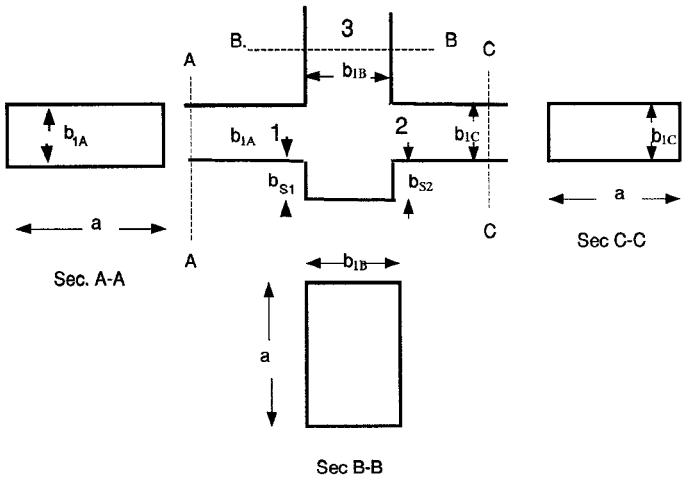

Fig. 1. Stepped E-plane and H-plane waveguide T-junction.

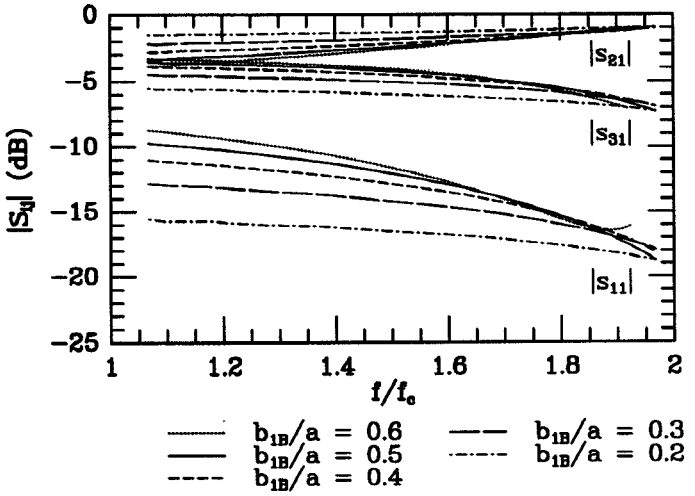

Fig. 2. *S*-parameters of E-plane T-junction with $b_{1A}/a = b_{1C}/a = 0.5$ and $b_{s1} = b_{s2} = 0$, and b_{1B}/a as a parameter.

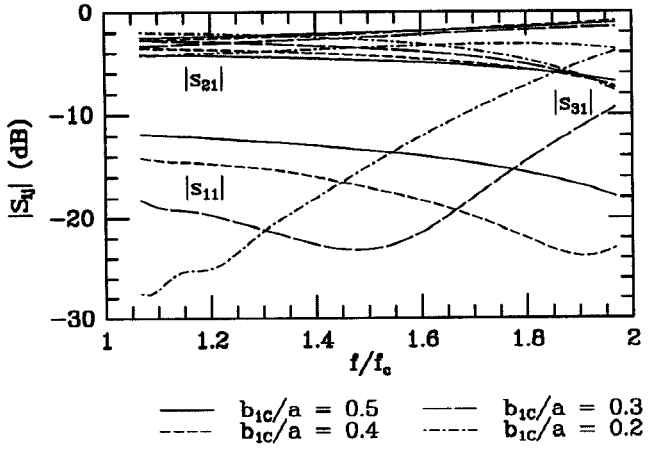

Fig. 3. *S*-parameters of E-plane T-junction with $b_{1A}/a = 0.5$, $b_{1B}/a = 0.35$, $(b_{1c} + b_{s2})/a = 0.5$, and $b_{s1} = 0$, and b_{1C}/a as a parameter.

An optimum design was similarly obtained for the H-plane T-junction. To maintain the same cutoff frequency, the dimensions b_{1A}, b_{1B}, and b_{1C} could not be varied (note that b's are larger than a for the H-plane

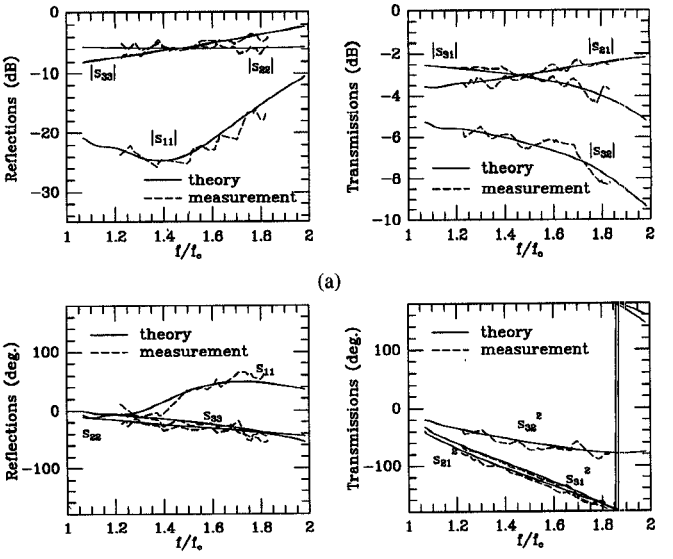

Fig. 4. Measured results of an E-plane T-junction with optimized dimensions compared to theory. (a) Amplitude, (b) phase. T-junction dimensions $a = 0.9$, $b_{1A} = 0.4$, $b_{1C} = 0.21$, $b_{1B} = 0.275$, $b_{s1} = 0$, and $b_{s2} = 0.19$ (all dimensions in inches).

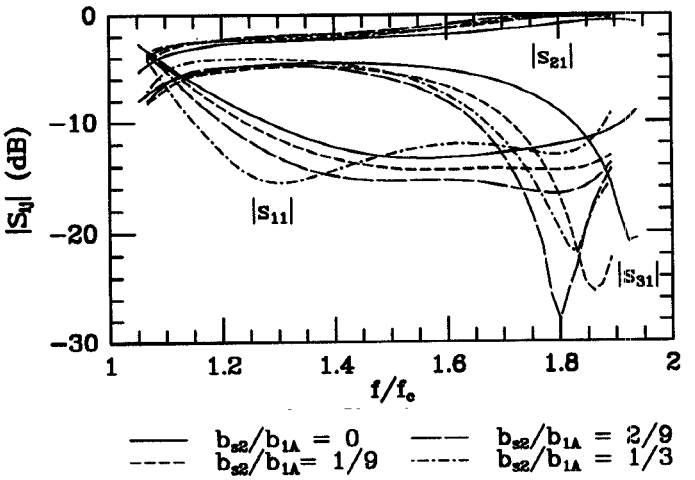

Fig. 5. *S* parameters of H-plane T-junction with $b_{1A}/a = b_{1C}/a = b_{1B}/a = 2.0$ and $b_{s1} = 0$, and b_{s2}/b_{1A} as a parameter.

T-junction). Consequently, only steps b_{s1} and b_{s2} can be used for optimization keeping b_{1A}, b_{1B}, and b_{1C} fixed. Fig. 5 shows the results of H-plane T-junctions with different steps in port 2. It is clear by comparing Figs. 4 and 5 that the E-plane T-junction has a performance superior to H-plane T-junction for wide-band application.

B. Ridge Waveguide Stepped T-Junction

The ridge waveguide T-junction shown in Fig. 6 consists of three ridge waveguide regions of different cross section. Regions A, C, and B are ridge guides with cross sections $a \times b_{1A}$, $a \times b_{1C}$, and $a \times (b_{1A} + b_{s1} + l_i)$, respectively, where l_i are the distances of the short circuits from the port 3 reference plane. The ridge cross sections are $w \times h_i$, where h_i, $i = 1, 2, 3$ are the heights of the ridge in regions A, B, and C, respectively. Normal modes can be found for each region. This is done by the

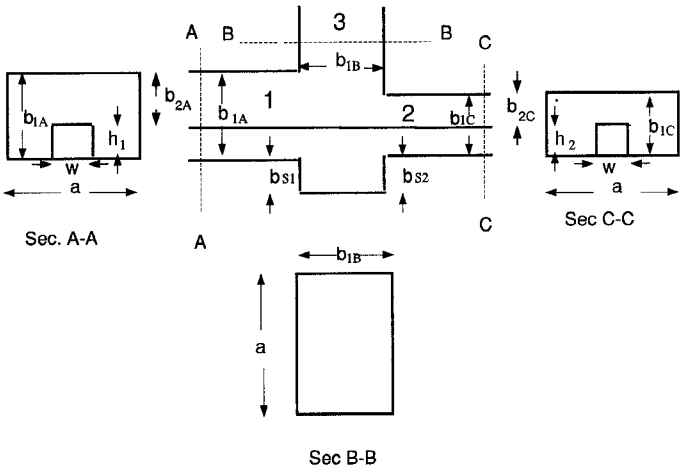

Fig. 6. Stepped E-plane ridge waveguide T-junction.

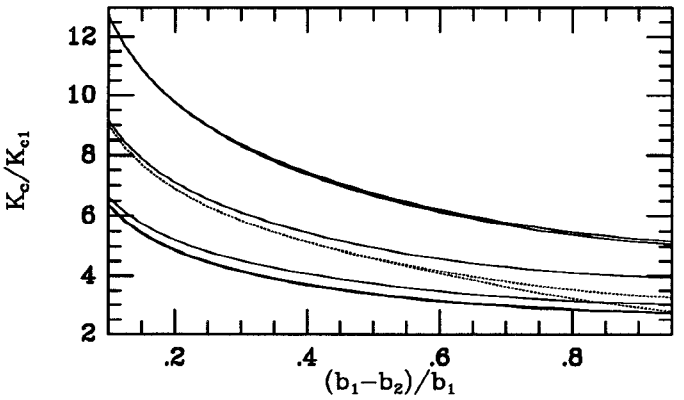

Fig. 7. Normalized mode chart of the ridge waveguide showing the cutoff wave number of the higher order modes normalized to that of the fundamental.

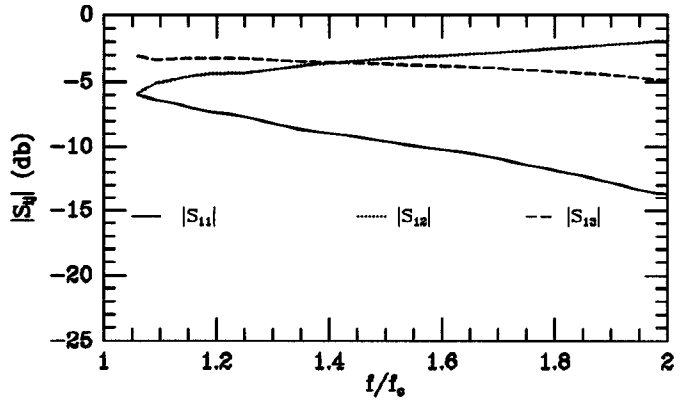

Fig. 8. Ridge waveguide T-junction before optimization with $a = 1.872$, $b_{1A} = b_{1C} = b_{1B} = 0.872$, $b_{s1} = b_{s2} = 0$, $b_{2A} = b_{2C} = 0.472$, and $w = 0.18$ (all dimensions in inches).

mode matching and formulation given in the Appendix. Then the scattering matrix characterizing the discontinuity between ridge waveguides of different cross sections is determined also by mode matching.

Fig. 7 is a mode chart showing the ridge waveguide normalized cutoff wave number versus $(b_1 - b_2/b_1)$ (refer to Fig. 17). Fig. 8 shows S-parameters of an unoptimized ridge T-junction. For optimization, several approaches have been investigated. Fig. 9 shows the results of symmetrical T-junction. The best configuration was obtained with unsymmetrical steps in both input and output arms, and the results are shown in Fig. 10. The bandwidth for the optimum ridge waveguide stepped T-junction is considerably wider than the regular waveguide stepped T-junction.

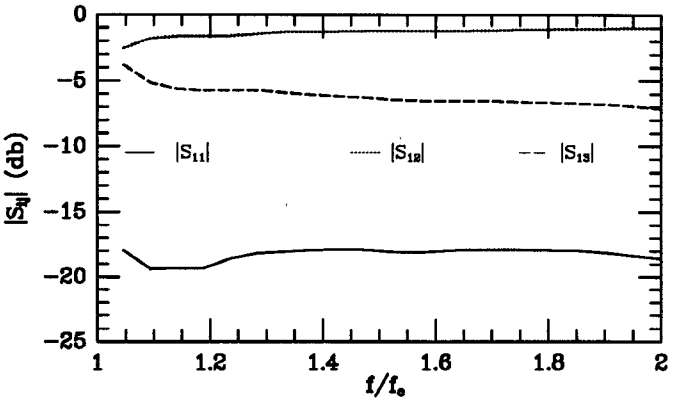

Fig. 9. Ridge waveguide T-junction after optimization with $a = 1.872$, $b_{1A} = 0.672$, $b_{1C} = 0.672$, $b_{1B} = 0.2$, $b_{s1} = b_{s2} = 0.2$, $b_{2A} = 0.272$, $b_{2C} = 0.272$, and $w = 0.18$ (all dimensions in inches).

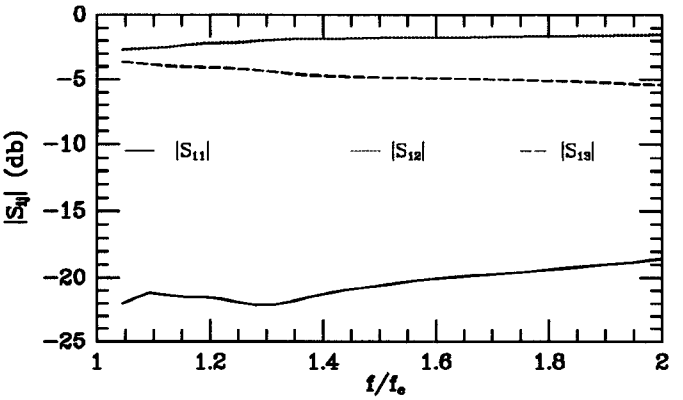

Fig. 10. Ridge waveguide T-junction after optimization with $a = 1.872$, $b_{1A} = 0.672$, $b_{1C} = 0.672$, $b_{1B} = 0.2$, $b_{s1} = 0.2$, $b_{s2} = 0$, $b_{2A} = 0.472$, $b_{2C} = 0.272$, and $w = 0.18$ (all dimensions in inches).

III. Diplexer Modeling and Optimization

Typical requirements of a broad-band diplexer are given in Table I. Broad-band diplexers using snaked stripline and printed circuit elements were reported in [4]–[6]. These types of diplexers provide less than 15 dB passband return loss, have relatively high insertion loss, and cannot handle high power. To achieve the high-quality requirements, waveguide-type diplexers are the most suitable configuration. Previous waveguide diplexers reported in [7] and [8] are narrow-band.

The diplexer network model, shown in Fig. 11, consists of two bandpass filters connected to ports 2 and 3 of the optimized T-junction whose response is shown in Fig. 12. Initial filter designs were chosen as inductive windows, doubly terminated, 0.01 dB ripple Chebyshev filters of orders 13 and 9.

TABLE I
BROAD-BAND DIPLEXER REQUIREMENTS

Parameter	Requirements
Channel 1 passband	3.52–4.2 GHz
Channel 2 passband	4.35–5.0 GHz
Min. passband return loss	>22 dB
Max. passband insertion loss	0.25 dB
Min. passband insertion loss (Ch. 1)	>20 dB, 4.35–5.0 GHz
Min. passband insertion loss (Ch. 2)	>20 dB, 3.52–4.2 GHz
Power handling capability (CW)	Min. 1 KW for each channel

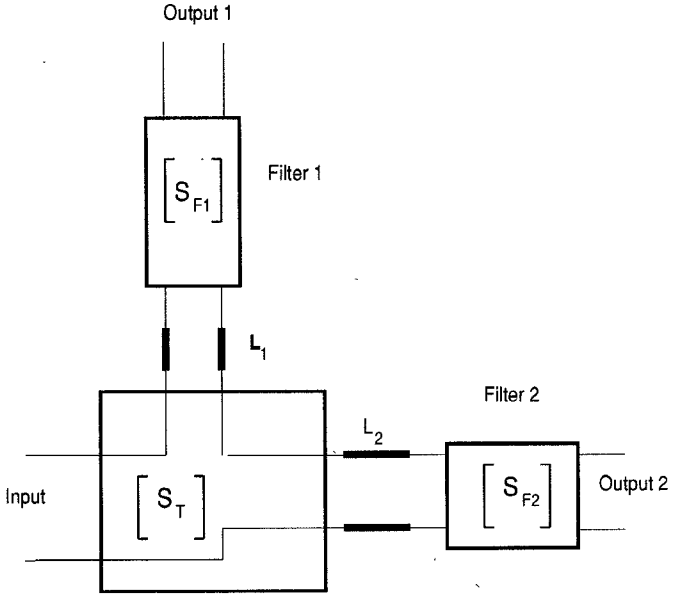

Fig. 11. The diplexer configuration consisting of T-junction, two filters, and two pieces of connecting waveguides.

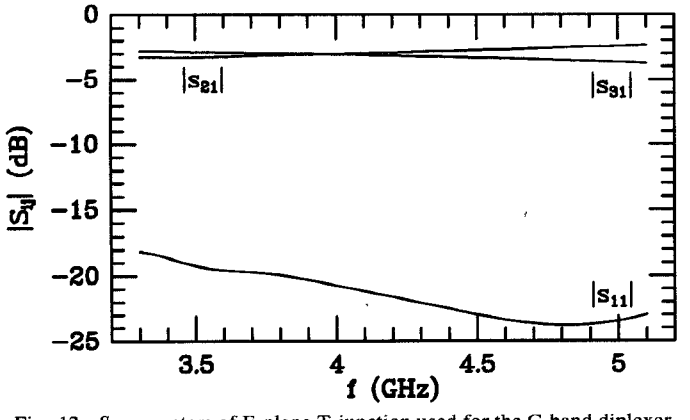

Fig. 12. *S*-parameters of E-plane T-junction used for the C-band diplexer, with $a = 1.872$, $b_{1A} = 0.872$, $b_{1C} = 0.522$, $b_{1B} = 0.6$, $b_{s1} = 0$, $b_{s2} = 0.35$ (all dimensions in inches).

A. Filter Modeling

The channel filters are modeled by their *S*-parameters. These *S*-parameters are computed by cascading the *S*-parameter matrices of each individual window and the lengths of waveguides forming the resonators. Each inductive window can be modeled as a lossless reciprocal junction with a scattering matrix as shown in Fig. 13(a). A circuit representation of the junction as a cascade of an ideal inverter and two sections of transmission lines is possible and is shown in Fig. 13(b).

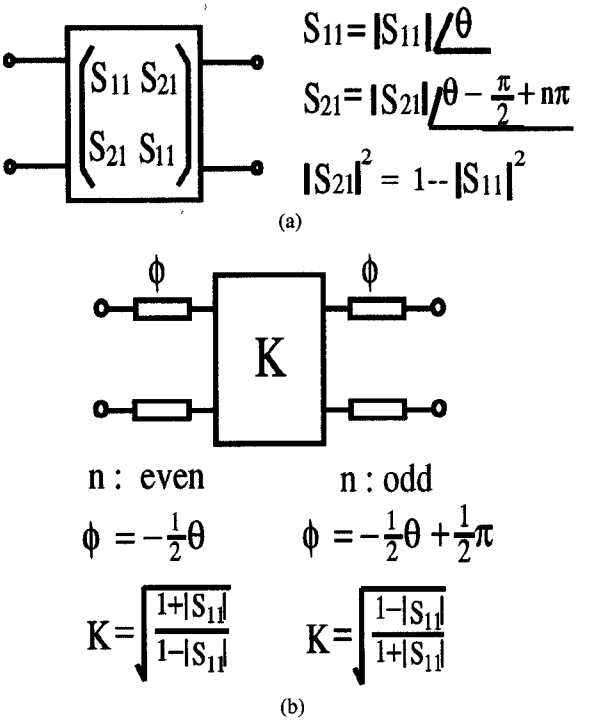

Fig. 13. (a) Scattering matrix of a lossless, symmetrical reciprocal junction; (b) is a circuit representation of (a).

The *S*-parameters (or values of k and ϕ) of the inductive window are evaluated by mode matching, and are found to be well-behaved functions of frequency f and window width w when the thickness t is fixed. Using this property, k and ϕ are computed at some sample points (w, f), then a two-dimensional curve fitting technique is used to get approximate polynomial representation of k and ϕ given by [9]

$$K(w,f) = \sum_{n=0}^{N} \sum_{m=0}^{M} k_{mn} f^m \left(\frac{w}{L_a}\right)^n \tag{1}$$

$$\phi(w,f) = \sum_{n=0}^{N} \sum_{m=0}^{M} \phi_{mn} f^m \left(\frac{w}{L_a}\right)^n \tag{2}$$

where L_a is the waveguide width, k_{mn} and ϕ_{mn} can be found from the values of k and ϕ at the grid points (f, w) computed from mode matching. The results are given in Fig. 14. The two-dimensional polynomial approximations are very useful for the optimization, since they reduce the computing time by several orders of magnitude without degradation of accuracy.

B. Diplexer Optimization

Since the required bandwidth of the diplexer is relatively wide, optimization of the filters and their spacing on the optimized T-junction are essential. Assume the required specification for the common port return loss to be $R_s(f_i)$ dB, the insertion loss between the input common

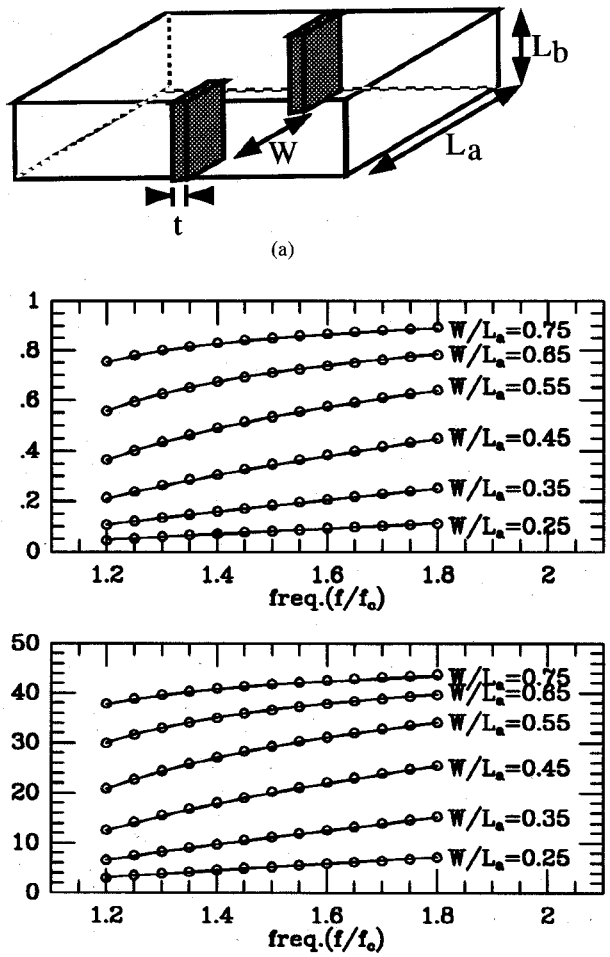

Fig. 14. (a) Configuration of an inductive window; (b) the element values of the circuit representation computed by mode matching and curve fitting. $L_a = 2.0\ L_b$, $t = 0.135 L_a$.

port and the diplexer output ports to be $T_{s1}(f_i)$ and $T_{s2}(f_i)$ dB $i = 1,2, \cdots, N$ where f_i are frequency points, then the objective function of the optimization is constructed as

$$R_{err} = \left\{ \frac{1}{N} \left(\sum_{i=1}^{N} \delta_i^p \right) + \frac{w_1}{N} \left(\sum_{i=1}^{N} \delta_{T_{1i}}^p \right) + \frac{w_2}{N} \left(\sum_{i=1}^{N} \delta_{T_{2i}}^p \right) \right\}^{(1/2)} \tag{3}$$

where

$$\delta_i = \begin{cases} R(f_i\{x\}) - R_s(f_i) & (R(f_i,\{x\}) - R_s(f_i) > 0) \\ 0 & (R(f_i,\{x\}) - R_s(f_i) < 0) \quad (f_i \in \text{pass band}) \\ wR(f_i,\{x\}) & (f_i \in \text{the stopband}) \end{cases}$$

$$\delta_{T_{1i}} = \begin{cases} T_1(f_i\{x\}) - T_{s1}(f_i) & T_1(f_i,\{x\}) - T_{s1}(f_i) > 0 \\ 0 & T_1(f_i,\{x\}) - T_{s1}(f_i) < 0 \end{cases} \quad (f_i \in \text{channel 1 stopband})$$

$$\delta_{T_{2i}} = \begin{cases} T_2(f_i\{x\}) - T_{s2}(f_i) & T_2(f_i,\{x\}) - T_{s2}(f_i) > 0 \\ 0 & T_2(f_i,\{x\}) - T_{s2}(f_i) < 0 \end{cases} \quad (f_i \in \text{channel 2 stopband}).$$

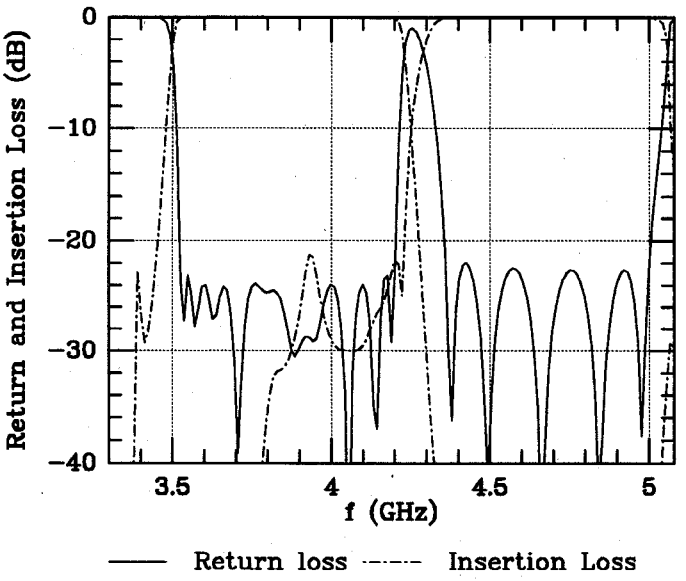

Fig. 15. Design results of the C-band diplexer (solid lines—return loss, dotted lines—insertion loss).

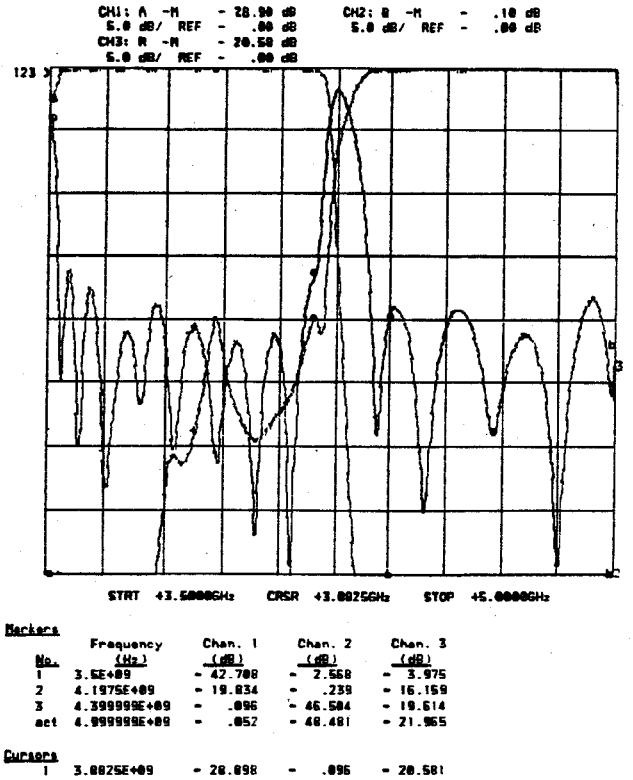

Fig. 16. Measured response of the C-band diplexer.

$R(f_i, \{x\})$, $T_1(f_i, \{x\})$, and $T_2(f_i, \{x\})$ are the computed return loss at the common port, and the insertion losses from the common port to the diplexer output ports 1 and 2 in dB, respectively, for a set of parameters $\{x\}$ of the filters and their spacings in the T-junction. $w > 1$ is a weighting coefficient chosen between 50 and 100, p is a weighting power factor chosen to be 2 in the initial stages of optimizations and 4 in the final stages. w_1 and w_2 are weighting coefficients chosen between 0 and 1.

The reflection and transmission coefficients of the diplexer are computed by cascading the S-parameters of the filters and the T-junction. Fig. 15 shows the optimized diplexer response, while Fig. 16 gives the measured diplexer response.

IV. Conclusion

A procedure for the design of wide-band T-junction diplexers is described. The properties of E-plane and H-plane waveguide and ridge waveguide step T-junctions are analyzed. It is found that the E-plane T-junction has performance superior to the H-plane T-junction for wide-band applications. The curve fitting procedure of two-dimensional polynomials to the electrical parameters of inductive windows, which are used in the filters and are computed by rigorous mode matching, is presented. This procedure, used in the diplexer optimization, dramatically reduces the required computational time without sacrificing accuracy. A wide-band 3-dB T-junction, which is an important component in the design of the wide-band diplexer, is optimized and verified by measurement. An optimization model for the wide-band diplexer is implemented. Using this model, a C-band T-junction waveguide diplexer, with total 31% bandwidth and return loss better than 22 dB in passbands, is designed. Experimental measurements on the diplexer showed excellent agreement with the design without any tuning.

Appendix
Modes in Ridge Waveguides

The ridge waveguide is divided into two regions—I and II—as shown in Fig. 17. Assuming a magnetic wall at the center of the guide, the TE modes are given by the following.

For region I,

$$j\omega\mu H_{z1} = \sum_n A_{1n} \cos(k_{x1n}x) \cosh(k_{y1n}y) \tag{A1a}$$

$$E_{x1} = -\sum_n \frac{A_{1n}}{k_c^2} k_{y1n} \cos(k_{x1n}x) \sinh(k_{y1n}y) = j\omega\mu H_{y1} Z_{TE} \tag{A1b}$$

$$E_{y1} = -\sum_n \frac{A_{1n}}{k_c^2} k_{x1n} \sin(k_{x1n}x) \cosh(k_{y1n}y) = -j\omega\mu H_{x1} Z_{TE} \tag{A1c}$$

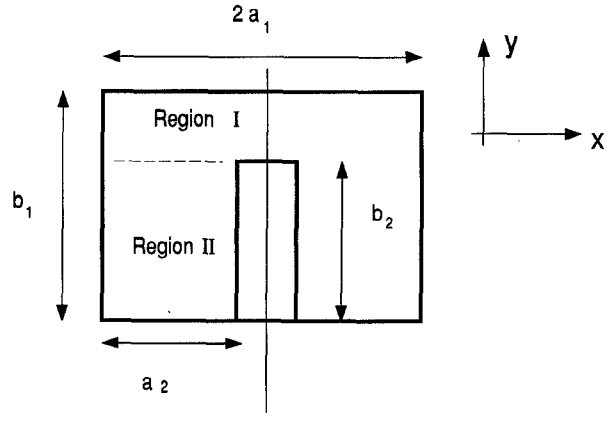

Fig. 17. Ridge waveguide cross section with magnetic wall at the line of symmetry.

where

$$k_{x1n}^2 - k_{y1n}^2 = \gamma^2 + k^2 = k_c^2 \tag{A1d}$$

$$k_{x1n} = \frac{(2n-1)\pi}{a_1}, \quad k^2 = \omega^2\mu\epsilon, \quad Z_{TE} = \frac{1}{\gamma} \tag{A1e}$$

γ, k_c, and Z_{TE} are the propagation constant, the cutoff wave number, and the wave impedance, respectively.

For region II,

$$j\omega\mu H_{z2} = \sum_m B_{2m} \cos(k_{x2m}x) \cosh(k_{y2m}(y - b_{1B})) \tag{A2a}$$

$$E_{x2} = -\sum_m \frac{B_{2m}}{k_c^2} k_{y2m} \cos(k_{x2m}x) \sinh(k_{y2m}(y - b_{1B})) = j\omega\mu H_{y2} Z_{TE} \tag{A2b}$$

$$E_{y2} = -\sum_m \frac{B_{2m}}{k_c^2} k_{x2m} \sin(k_{x2m}x) \cosh(k_{y2m}(y - b_{1B})) = -j\omega\mu H_{x2} Z_{TE} \tag{A2c}$$

where

$$k_{x2m}^2 - k_{y2m}^2 = \gamma^2 + k^2 = k_c^2 \tag{A2d}$$

$$k_{x2m} = \frac{m\pi}{a_2}. \tag{A2e}$$

By applying the boundary conditions at $y = b_{2B}$, taking the inner products, and using the orthogonality relations on the eigenfields in each region, the following characteristic equation is obtained:

$$\det[X] = 0 \tag{A3}$$

where X is an $(N \times N)$ matrix, and N is the number of eigenmodes used in region I. The elements of the matrix

X are

$$x_{ij} = \cosh(k_{y1j}b_{2B}) \sum_{m=0}^{M} [T_m k_{y2m} \tanh(k_{y2m}(b_{2B} - b_{1B})) \cdot \langle \hat{e}_{2m}, \hat{h}^*_{1j} \rangle \langle \hat{e}_{2m}, \hat{h}^*_{1i} \rangle] - \delta_{ij} \frac{a_1 a_2}{4T_i} k_{y1i} \sinh(k_{y1i}b_{2B}) \quad \text{(A4a)}$$

$$T_m = \begin{cases} 1, & m \neq 0 \\ \frac{1}{2}, & m = 0 \end{cases}, \quad \delta_{ij} = \begin{cases} 0, & i \neq j \\ 1, & i = j \end{cases} \quad \text{(A4b)}$$

where $(M + 1)$ is the number of modes used in region II.

The inner product are defined as

$$\langle \hat{e}, \hat{h}^* \rangle = \int_S \hat{e} \times \hat{h}^* \cdot \hat{a}_z \, dS$$

where S is the waveguide cross section.

Solving (A3), a group of eigenvalues of γ's can be obtained. Each γ corresponds to a TE mode in the ridge waveguide.

A similar formulation can be obtained for the TM case.

Acknowledgment

The authors would like to thank Dr. A. M. K. Saad of Scientific Microwave Corp., Ont., Canada, for his valuable suggestions and participation in this project.

References

[1] X.-P. Liang, K. A. Zaki, and A. E. Atia, "A rigorous three plane mode-matching technique for characterizing waveguide T-junctions, and its application in multiplexer design," *IEEE Trans. Microwave Theory Tech.*, vol. MTT-39, pp. 2138–2147, Dec. 1991.

[2] F. Arndt, I. Ahrens, U. Papziner, U. Wiechmann, and R. Wilkeit, "Optimized E-plane T-junction series power dividers," *IEEE Trans. Microwave Theory Tech.*, vol. MTT-35, pp. 1052–1059, Nov. 1987.

[3] J. P. Montgomery, "On the complete eigenvalue solution of ridged waveguide," *IEEE Trans. Microwave Theory Tech.*, vol. MTT-19, pp. 547–555, June 1971.

[4] M. Miyazaki, H. Asao, and O. Ishida, "A broad dielectric diplexer using a snaked strip-line," in *1991 IEEE MTT-S Dig.*, pp. 551–554.

[5] C. Nguyen and K. Chang, "W-band wideband low loss planar integrated circuit diplexer," *Microwave J.*, vol. 28, pp. 157–161, July 1985.

[6] Y.-C. Shih, L. Q. Bui, and T. Itoh, "Millimeter-wave diplexers with printed circuit elements," *IEEE Trans. Microwave Theory Tech.*, vol. MTT-33, pp. 1465–1469, Dec. 1985.

[7] J. Dittloff and F. Arndt, "Computer-aided design of slit-coupled H-plane T-junction diplexers with E-plane metal-insert filters," *IEEE Trans. Microwave Theory Tech.*, vol. MTT-36, pp. 1833–1840, Dec. 1988.

[8] J. L. Haine and J. D. Rhodes, "Direct design formulas for asymmetric bandpass channel diplexers," *IEEE Trans. Microwave Theory Tech.*, vol. MTT-25, pp. 807–814, Oct. 1977.

[9] J.-F. Liang and K. A. Zaki, "CAD of microwave junctions by polynomial curve fitting," in *1993 IEEE MTT-S Int. Microwave Symp. Dig.*

Hui-Wen Yao (S'93) was born in Inner Mongolia, China, in 1962. He received the B.S. and M.S. degrees, both in electrical engineering, from Beijing Institute of Technology, Beijing, China, in 1983 and 1986, respectively.

From 1986 to 1991 he was a Lecturer in the Department of Electrical Engineering, Beijing Institute of Technology, where his research dealt mainly with EM radiation, scattering, and antenna design. From 1991 to 1992 he was a Teaching Assistant in the Electrical Engineering Department, Wright State University, Dayton, OH, where he worked on transient scattering by cylinders. Presently he is a Research Assistant in the Microwave Lab, Department of Electrical Engineering, University of Maryland, College Park, working toward the Ph.D. degree. His current research interests include analysis, modeling, and design of microwave and millimeter-wave devices and circuits.

Amr E. Abdelmonem was born in Egypt on May 8, 1965. He received the B.Sc. (honors) and M.S. degrees from Ain-Shams University in 1987 and 1990, respectively.

From 1987 to 1990 he worked as a Teaching Assistant at Ain-Shams University. Since 1990 he has been a Research Assistant at the Department of Electrical Engineering, University of Maryland, where he is currently working toward the Ph.D. degree. His research interests include design of MIC, numerical methods in electromagnetics, and semiconductor lasers.

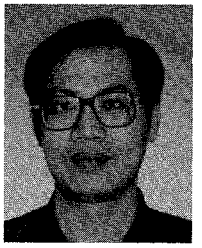

Ji-Fuh Liang was born in Taiwan, R.O.C., on November 25, 1958. He received the B.S. degree in electronics engineering from National Chiao-Tung University, Taiwan, in 1981, and the M.S. degree in electrical engineering from National Taiwan University, Taiwan, in 1985.

During 1981–1983 he was with the China military as a member of the technical staff. From 1985 to 1988 he was a member of technical staff and Project Leader at Microelectronics Technology Inc., Hsin-Chun, Taiwan. Since 1989 he has been working as a Research Assistant in the Microwave Lab, Department of Electrical Engineering, University of Maryland, College Park. Currently he is working toward the Ph.D. degree. His research interests include theoretical and experimental characterizations of microwave/millimeter-wave passive and active devices.

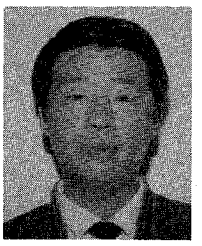

Xiao-Peng Liang (S'90) was born in Shanxi, China, in 1960. He received the B.S. and M.S. degrees from Beijing Institute of Technology, Beijing, China, in 1982 and 1984, respectively, both in electrical engineering.

From 1984 to 1987 he worked in the Electrical Engineering Department, Beijing Institute of Technology, as a faculty member, where his research dealt mainly with the six-port measurement technique. Now, he is a graduate student in the Electrical Engineering Department, University of Maryland, College Park, working toward the Ph.D. degree. His research interests are in the area of modeling and designing microwave and millimeter-wave waveguides, devices, and circuits. He will soon be a Staff Engineer at Antenna Specialist Co. Reno, NE.

Kawthar A. Zaki (SM'85–F'91) received the B.S. degree with honors from Ain Shams University, Cairo, Egypt, in 1962, and the M.S. and Ph.D. degrees from the University of California, Berkeley, in 1966 and 1969, respectively, all in electrical engineering.

From 1962 to 1964 she was a Lecturer in the Department of Electrical Engineering, Ain Shams University. From 1965 to 1969 she held the position of Research Assistant in the Electronic Research Laboratory, University of California, Berkeley. She joined the Electrical Engineering Department, University of Maryland, College Park, in 1970, where she is presently Professor of Electrical Engineering. Her research interests are in the areas of electromagnetics, microwave circuits, optimization, computer-aided design, and optically controlled microwave and millimeter-wave devices.

Alain Martin, photograph and biography not available at the time of publication.